AIMS Mathematics, 8(3): 6804–6828.
DOI: 10.3934/math.2023346
Received: 22 October 2022
Revised: 24 December 2022
Accepted: 03 January 2023
Published: 09 January 2023

http://www.aimspress.com/journal/Math

Research article

Two-dimensional discrete-time laser model with chaos and bifurcations

Abdul Qadeer Khan[1,*] **and Mohammed Bakheet Almatrafi**[2]

[1] Department of Mathematics, University of Azad Jammu and Kashmir, Muzaffarabad 13100, Pakistan

[2] Department of Mathematics, College of Science, Taibah University, Al-Madinah Al-Munawarah, Saudi Arabia

* **Correspondence:** Email: abdulqadeerkhan1@gmail.com; Tel: 00923445102758.

Abstract: We explore the local dynamical characteristics, chaos and bifurcations of a two-dimensional discrete laser model in $\mathbb{R}^2_+$. It is shown that for all a, b, c and p, model has boundary fixed point $P_{0y}(0, \frac{p}{c})$, and the unique positive fixed point $P^+_{xy}(\frac{ap-bc}{ab}, \frac{b}{a})$ if $p > \frac{bc}{a}$. Further, local dynamical characteristics with topological classifications for the fixed points $P_{0y}(0, \frac{p}{c})$ and $P^+_{xy}(\frac{ap-bc}{ab}, \frac{b}{a})$ have explored by stability theory. It is investigated that flip bifurcation exists for the boundary fixed point $P_{0y}(0, \frac{p}{c})$, and also there exists a flip bifurcation if parameters vary in a small neighborhood of the unique positive fixed point $P^+_{xy}(\frac{ap-bc}{ab}, \frac{b}{a})$. Moreover, it is also explored that for the fixed point $P^+_{xy}(\frac{ap-bc}{ab}, \frac{b}{a})$, laser model undergoes a Neimark-Sacker bifurcation, and in the meantime stable invariant curve appears. Numerical simulations are implemented to verify not only obtain results but also exhibit complex dynamics of period -2, -3, -4, -5, -8 and -9. Further, maximum lyapunov exponents along with fractal dimension are computed numerically to validate chaotic behavior of the laser model. Lastly, feedback control method is utilized to stabilize chaos exists in the model.

Keywords: laser model; bifurcation; chaos control; numerical simulations
Mathematics Subject Classification: 39A33, 37G35, 39A30, 37D45

1. Introduction

Differential and difference equations govern a wide range of physical models. In recent years, discrete models represented by difference equations have been better examined than continuous models. During the last few decades, mathematical models of physics, ecology, engineering, physiology, psychology, chemistry and social sciences have given birth to key research areas. Furthermore, like the biological model, physical model plays an active role in all fields of engineering and science; particularly laser model having enormous applications such as in industries for

manufacturing purposes, e.g., for drilling, welding, cutting, marking, hardening, ablating, engraving and micromachining etc. The lasers can also be utilized for the applications of optical data storage, e.g., in DVDs and compact disks (CDs) etc. With regard to communications, the lasers are employed for long-distance optical data transmission, e.g., for inter-satellite communications. On medical side, the lasers are used for vision correction (LASIK) and eye surgery, dermatology, dentistry (e.g., photodynamic therapy of cancer). In optical metrology, it is used for extremely precise position measurements and optical surface profiling. Similarly, in energy technology, it is used for electricity generation and laser-induced nuclear fusion etc. Moreover, in recent times few high-power lasers are developed for potential use as directed energy weapons in the battle field or for destroying missiles, mines and projectiles etc. [1–7].

The term laser is used for the phenomena of light production by emission of radiation. Laser is an appliance that is used for the production of coherent and single wavelength of light called monochromatic light. The basic principle for the working of laser based upon the theory of light proposed by Einstein in 1916, and developed by G. Gould in 1957. The first working ruby laser was introduced in 1960 by Theodore Maiman. One can differentiate laser light from ordinary light easily as it is very directional and monochromatic, and works on the principles of spontaneous emission, spontaneous absorption, population inversion and stimulated emission of the light. In nature, an atom exists in different energy states, when it absorb light it jumps from low energy state E_1 to higher energy state E_2. This condition is known as spontaneous absorption. Spontaneous emission represents the state of an atom as in excited state E_2 it does not remains for a long period of the time about 10^{-8} is a life time of an atom in a excited state and it jumps down from level E_2 to the lower lever E_1 by loosing energy in the form of photon of energy $h(v)$ is incoherent and moves in any direction. During this situation if another photon interacts with another atom which is in excited state, then it emits a pair of photon in same direction and same phase, and again it goes to its ground state. For the laser formation, it is necessary to amplify light in the cavity. For achieving population inversion, the atoms of gain medium accelerate to the high energy state by means of pumping. The chain of photon in cavity is obtained by population inversion and this chain become so intense that at the end of cavity reflected mirror cannot reflect them, and hence laser is obtained [8]. So, now we will give the mathematical formulation of the desired two-dimensional discrete-time laser model. As it is pointed out in [8], the number of laser photons in the cavity changes mainly for the following two reasons:

(i) Due to stimulated emission, laser photons are continuously being added.
(ii) Mirror transmission, absorption or scattering at the mirrors result continuously lost of laser photons.

Thus, the rate of change of number of laser photon including loss and gain represented by the equation as follows:

$$\frac{dx}{dt} = gain - loss = axy - bx. \tag{1.1}$$

The two rates, the rate of increase by means of stimulated emission as well as the rate of decrease by means of imperfect mirror indicates the rate at which the number of laser photons changes. In Eq (1.1), x denotes number of laser photon, y is number of atom in excited state, a is gain coefficient and b is the transmission coefficient. Moreover, equation (1.1) represents that due to stimulated emission the gain of laser photon is not only proportional to the number of photons already in cavity but also to the

number of atoms. Thus, the type of atom used and other factors collectively indicate the efficiency of the stimulated emission while the rate of loss of laser photon is simplify proportional to the number of laser photon present. Now, one has the following equation for y, that is, the number atom in excited state where both spontaneous and emission causes y to decrease, and the pump p causes y to increase at some rate

$$\frac{dy}{dt} = -axy - cy + p, \tag{1.2}$$

where c is the spontaneous emission. Note that with opposite sign the first term appears in both Eqs (1.1) and (1.2). This shows the increase of x corresponds precisely to the decrease of y and represents the role of stimulated emission in laser. Furthermore, equations (1.1) and (1.2) describe the laser action. These equations show the relation of number of laser photon in the cavity and the number of loosing atoms but do not indicate what happens to the atoms when their electrons jumps to some other level or the photons that leave the cavity. So, equations (1.1) and (1.2) give the following model equations of two-dimensional continuous-time laser model [8–10]:

$$\frac{dx}{dt} = axy - bx, \ \frac{dy}{dt} = -axy - cy + p. \tag{1.3}$$

Now, by Euler's forward scheme, the continuous-time laser model (1.3) becomes

$$x_{n+1} = (1 - bh)\, x_n + ahx_n y_n, \ y_{n+1} = (1 - ch)\, y_n - ahx_n y_n + ph. \tag{1.4}$$

The goal of this paper is to investigate local dynamical properties, chaos and bifurcations of the laser model (1.4). Precisely the rest of the paper is structured as follows: Linearized form and existence for the fixed points of the laser model (1.4) are explored in Section 2. In Section 3, local dynamics for the fixed points of the laser model (1.4) is explored. The existence of bifurcation for the fixed points is explored in Section 4. The detailed bifurcation analysis for the fixed points is explore in Section 5. In Section 6, theoretical results are verified numerically, and this also includes to study the fractal dimension. In Section 7, chaos control is investigated by feedback control method. Brief summary of the paper is presented in Section 8.

2. Equilibrium points and linearized form of the laser model (1.4)

Lemma 2.1. *Laser model (1.4) has at most two equilibria in $\mathbb{R}^2_+$. More specifically,*

(i) Laser model (1.4) has a boundary fixed point $P_{0y}\left(0, \frac{p}{c}\right)$ $\forall$ a, b, c, p, h;

(ii) Laser model (1.4) has an interior fixed point $P^+_{xy}\left(\frac{ap-bc}{ab}, \frac{b}{a}\right)$ if $p > \frac{bc}{a}$.

Hereafter, for the fixed point $P_{xy}(x^*, y^*)$, linearized form is explored. The linearized system of (1.4) for the fixed point $P_{xy}(x^*, y^*)$ under the map $(\Phi_1, \Phi_2) \to (x_{n+1}, y_{n+1})$ is

$$\Gamma_{n+1} \quad = \quad J|_{(x^*, y^*)}\Gamma_n, \tag{2.1}$$

where

$$J|_{(x^*, y^*)} := \begin{pmatrix} 1 - bh + ahy^* & ahx^* \\ -ahy^* & 1 - ch - ahx^* \end{pmatrix}, \tag{2.2}$$

and

$$\Phi_1 = (1 - bh)\, x_n + ahx_n y_n, \ \Phi_2 = (1 - ch)\, y_n - ahx_n y_n + ph. \tag{2.3}$$

3. Local dynamics for the fixed points of laser model (1.4)

Local dynamics for the fixed points $P_{0y}\left(0, \frac{p}{c}\right)$ and $P^{+}_{xy}\left(\frac{ap-bc}{ab}, \frac{b}{a}\right)$ of (1.4) is explored in this section, as follows.

3.1. Local dynamics for $P_{0y}\left(0, \frac{p}{c}\right)$

The $J|_{P_{0y}\left(0,\frac{p}{c}\right)}$ evaluated at $P_{0y}\left(0, \frac{p}{c}\right)$ is

$$J|_{P_{0y}\left(0,\frac{p}{c}\right)} = \begin{pmatrix} 1 - bh + \frac{aph}{c} & 0 \\ -\frac{aph}{c} & 1 - ch \end{pmatrix}. \tag{3.1}$$

The roots of $J|_{P_{0y}\left(0,\frac{p}{c}\right)}$ evaluated at $P_{0y}\left(0, \frac{p}{c}\right)$ are $\lambda_1 = 1 - bh + \frac{aph}{c}$ and $\lambda_2 = 1 - ch$. So, by stability theory, dynamics of (1.4) for $P_{0y}\left(0, \frac{p}{c}\right)$ can be stated, as follows.

Lemma 3.1. *For $P_{0y}\left(0, \frac{p}{c}\right)$, following statements hold:*

(i) $P_{0y}\left(0, \frac{p}{c}\right)$ of the laser model (1.4) is a sink if

$$p > \frac{bch - 2c}{ah} \text{ and } c < \frac{2}{h}; \tag{3.2}$$

(ii) $P_{0y}\left(0, \frac{p}{c}\right)$ of the laser model (1.4) is a source if

$$p < \frac{bch - 2c}{ah} \text{ and } c > \frac{2}{h}; \tag{3.3}$$

(iii) $P_{0y}\left(0, \frac{p}{c}\right)$ of the laser model (1.4) is a saddle if

$$p < \frac{bch - 2c}{ah} \text{ and } c < \frac{2}{h}; \tag{3.4}$$

(iv) $P_{0y}\left(0, \frac{p}{c}\right)$ of the laser model (1.4) is non-hyperbolic if

$$p = \frac{bch - 2c}{ah} \text{ or } c = \frac{2}{h}. \tag{3.5}$$

3.2. Local dynamics for $P^{+}_{xy}(\frac{ap-bc}{ab}, \frac{b}{a})$

The $J|_{P^{+}_{xy}(\frac{ap-bc}{ab},\frac{b}{a})}$ evaluated at $P^{+}_{xy}(\frac{ap-bc}{ab}, \frac{b}{a})$ is

$$J|_{P^{+}_{xy}(\frac{ap-bc}{ab},\frac{b}{a})} = \begin{pmatrix} 1 & \frac{aph-bch}{b} \\ -bh & \frac{b-aph}{b} \end{pmatrix}. \tag{3.6}$$

The corresponding auxiliary equation of (3.6) is

$$\lambda^2 - p_1\lambda + q_1 = 0, \tag{3.7}$$

where

$$\begin{aligned} p_1 &= \frac{2b - aph}{b}, \\ q_1 &= \frac{b - aph}{b} + h^2 (ap - bc). \end{aligned} \tag{3.8}$$

Finally, the roots of (3.7) are

$$\lambda_{1,2} = \frac{p_1 \pm \sqrt{\Delta}}{2}, \tag{3.9}$$

where

$$\begin{aligned} \Delta &= \left(\frac{2b - aph}{b}\right)^2 - 4\left(\frac{b - aph}{b} + h^2 (ap - bc)\right) \\ &= \left(\frac{aph}{b}\right)^2 - 4h^2 (ap - bc). \end{aligned} \tag{3.10}$$

Hereafter, local dynamics for the fixed point $P^+_{xy}\left(\frac{ap-bc}{ab}, \frac{b}{a}\right)$ of the laser model (1.4) can be summarized according to the sign of $\Delta < 0$ ($\Delta \geq 0$), as follows.

Lemma 3.2. *If $\Delta = \left(\frac{aph}{b}\right)^2 - 4h^2 (ap - bc) < 0$, then for $P^+_{xy}\left(\frac{ap-bc}{ab}, \frac{b}{a}\right)$ of the laser model (1.4), following statements hold:*

(i) $P^+_{xy}\left(\frac{ap-bc}{ab}, \frac{b}{a}\right)$ is a locally asymptotically stable focus if

$$p < \frac{hb^2c}{a(bh - 1)}; \tag{3.11}$$

(ii) $P^+_{xy}\left(\frac{ap-bc}{ab}, \frac{b}{a}\right)$ is an unstable focus if

$$p > \frac{hb^2c}{a(bh - 1)}; \tag{3.12}$$

(iii) $P^+_{xy}\left(\frac{ap-bc}{ab}, \frac{b}{a}\right)$ is non-hyperbolic if

$$p = \frac{hb^2c}{a(bh - 1)}. \tag{3.13}$$

Lemma 3.3. *If $\Delta = \left(\frac{aph}{b}\right)^2 - 4h^2 (ap - bc) \geq 0$, then for $P^+_{xy}\left(\frac{ap-bc}{ab}, \frac{b}{a}\right)$ of the laser model (1.4), following statements hold:*

(i) $P^+_{xy}\left(\frac{ap-bc}{ab}, \frac{b}{a}\right)$ is a locally asymptotically stable node if

$$p < \frac{b\left(4 - bh^2c\right)}{ah(2 - bh)}; \tag{3.14}$$

(ii) $P^+_{xy}\left(\frac{ap-bc}{ab}, \frac{b}{a}\right)$ is an unstable node if

$$p > \frac{b\left(4 - bh^2c\right)}{ah(2 - bh)}; \tag{3.15}$$

(iii) $P^+_{xy}\left(\frac{ap-bc}{ab}, \frac{b}{a}\right)$ is non-hyperbolic if

$$p = \frac{b\left(4 - bh^2c\right)}{ah(2 - bh)}. \tag{3.16}$$

4. Existence of bifurcations for $P_{0y}\left(0, \frac{p}{c}\right)$ and $P^{+}_{xy}\left(\frac{ap-bc}{ab}, \frac{b}{a}\right)$ of the laser model (1.4)

(i) If (3.5) true then one of eigenvalues of $J|_{P_{0y}\left(0,\frac{p}{c}\right)}$ evaluated at $P_{0y}\left(0, \frac{p}{c}\right)$ is -1, *i.e.*, $\lambda_1|_{(3.5)} = -1$ but $\lambda_2|_{(3.5)} = 1 - ch \neq 1$ or -1. Thus, laser model (1.4) undergoes a flip bifurcation when (a, b, c, h, p) passes through the curve

$$FB|_{P_{0y}\left(0,\frac{p}{c}\right)} = \left\{(a, b, c, h, p),\ p = \frac{bch - 2c}{ah}\right\}; \tag{4.1}$$

(ii) If (3.13) true then roots of $J|_{P^{+}_{xy}\left(\frac{ap-bc}{ab},\frac{b}{a}\right)}$ evaluated at $P^{+}_{xy}\left(\frac{ap-bc}{ab}, \frac{b}{a}\right)$ satisfying $\left|\lambda_{1,2}\right|_{(3.13)} = 1$. Thus, laser model (1.4) undergoes Neimark-Sacker bifurcation when (a, b, c, h, p) passes through the curve

$$NSB|_{P^{+}_{xy}\left(\frac{ap-bc}{ab},\frac{b}{a}\right)} = \left\{(a, b, c, h, p),\ p = \frac{hb^2c}{a\,(bh - 1)}\right\}; \tag{4.2}$$

(iii) If (3.16) true then one of the eigenvalues of $J|_{P^{+}_{xy}\left(\frac{ap-bc}{ab},\frac{b}{a}\right)}$ evaluated at $P^{+}_{xy}\left(\frac{ap-bc}{ab}, \frac{b}{a}\right)$ is -1, *i.e.*, $\lambda_1|_{(3.16)} = -1$ but $\lambda_2|_{(3.16)} = \frac{2-3bh+bch^2}{2-bh} \neq 1$ or -1. So model (1.4) undergoes a flip bifurcation when (a, b, c, h, p) passes the curve

$$FB|_{P^{+}_{xy}\left(\frac{ap-bc}{ab},\frac{b}{a}\right)} = \left\{(a, b, c, h, p),\ p = \frac{b\left(4 - bch^2\right)}{ah\,(2 - bh)}\right\}. \tag{4.3}$$

5. Bifurcation analysis for fixed points $P_{0y}\left(0, \frac{p}{c}\right)$ and $P^{+}_{xy}\left(\frac{ap-bc}{ab}, \frac{b}{a}\right)$ of the laser model (1.4)

We study comprehensive bifurcation analysis for fixed points $P_{0y}\left(0, \frac{p}{c}\right)$ and $P^{+}_{xy}\left(\frac{ap-bc}{ab}, \frac{b}{a}\right)$ of the discrete model (1.4) in this section. This comprises the study of flip bifurcation for $P_{0y}(0, \frac{p}{c})$, Neimark-Sacker and flip bifurcations for $P^{+}_{xy}\left(\frac{ap-bc}{ab}, \frac{b}{a}\right)$ of the discrete laser model (1.4).

5.1. Flip bifurcation for $P_{0y}\left(0, \frac{p}{c}\right)$

Recall that for $P_{0y}\left(0, \frac{p}{c}\right)$, model (1.4) undergoes a flip bifurcation when (a, b, c, h, p) passes through the curve (4.1). But by calculation it can not occur, and therefore $P_{0y}\left(0, \frac{p}{c}\right)$ is degenerate with higher codimension.

5.2. Neimark-Sacker bifurcation for $P^{+}_{xy}\left(\frac{ap-bc}{ab}, \frac{b}{a}\right)$

Hereafter, we will give detail Neimark-Sacker bifurcation for $P^{+}_{xy}\left(\frac{ap-bc}{ab}, \frac{b}{a}\right)$ of (1.4) by utilizing bifurcation theory [11–13]. Recall that if (4.2) holds, then $|\lambda_{1,2}| = 1$. So, consider p in a small neighborhood of p^*, *i.e.*, $p = p^* + \epsilon$ where $\epsilon << 1$ and hence (1.4) gives

$$x_{n+1} = (1 - bh)x_n + ahx_ny_n,\ y_{n+1} = (1 - ch)y_n - ahx_ny_n + h(p^* + \epsilon). \tag{5.1}$$

The ϵ-dependence laser model (5.1) has fixed point $P^{+}_{xy}\left(\frac{a(p^{*}+\epsilon)-bc}{ab}, \frac{b}{a}\right)$ and the $J|_{P^{+}_{xy}\left(\frac{a(p^{*}+\epsilon)-bc}{ab}, \frac{b}{a}\right)}$ evaluated at $P^{+}_{xy}\left(\frac{a(p^{*}+\epsilon)-bc}{ab}, \frac{b}{a}\right)$ is

$$J|_{P^{+}_{xy}\left(\frac{a(p^{*}+\epsilon)-bc}{ab}, \frac{b}{a}\right)} = \begin{pmatrix} 1 & \frac{a(p^{*}+\epsilon)h-bch}{b} \\ -hb & \frac{b-a(p^{*}+\epsilon)h}{b} \end{pmatrix}. \tag{5.2}$$

The characteristic equation of $J|_{P^{+}_{xy}\left(\frac{a(p^{*}+\epsilon)-bc}{ab}, \frac{b}{a}\right)}$ evaluated at $P^{+}_{xy}\left(\frac{a(p^{*}+\epsilon)-bc}{ab}, \frac{b}{a}\right)$ is

$$\lambda^2 - p_1(\epsilon)\lambda + q_1(\epsilon) = 0, \tag{5.3}$$

where

$$\begin{aligned} p_1(\epsilon) &= \frac{2b - a(p^{*}+\epsilon)h}{b}, \\ q_1(\epsilon) &= \frac{b - a(p^{*}+\epsilon)h}{b} + h^2\left(a(p^{*}+\epsilon) - bc\right). \end{aligned} \tag{5.4}$$

The zeroes of (5.3) become

$$\lambda_{1,2} = \frac{p_1(\epsilon) \pm \iota\sqrt{4q_1(\epsilon) - p_1^2(\epsilon)}}{2}, \tag{5.5}$$

where

$$\begin{aligned} \Delta &= p_1^2(\epsilon) - 4q_1(\epsilon) \\ &= \left(\frac{a(p^{*}+\epsilon)h}{b}\right)^2 - 4h^2\left(a(p^{*}+\epsilon) - bc\right). \end{aligned} \tag{5.6}$$

Moreover after some computation, one has

$$\frac{d|\lambda_{1,2}|}{d\epsilon}|_{\epsilon=0} = \frac{bch}{2(bh-1)} \neq 0. \tag{5.7}$$

Additionally, it is required that $\lambda_{1,2}^{m} \neq 1,\ m = 1, \cdots, 4$, that is same to $p(0) \neq -2, 0, 1, 2$, and so it is true by calculation. Using following transformation:

$$u_n = x_n - x^{*}, v_n = y_n - y^{*}, \tag{5.8}$$

the fixed point $P^{+}_{xy}\left(\frac{a(p^{*}+\epsilon)-bc}{ab}, \frac{b}{a}\right)$ of system (5.1) transform into $P_{00}(0, 0)$. So, (5.1) becomes

$$\begin{aligned} u_{n+1} &= (1 - bh)(u_n + x^{*}) + ah(u_n + x^{*})(v_n + y^{*}) - x^{*}, \\ v_{n+1} &= (1 - ch)(v_n + y^{*}) - ah(u_n + x^{*})(v_n + y^{*}) + h(p^{*} + \epsilon) - y^{*}, \end{aligned} \tag{5.9}$$

where $x^{*} = \frac{a(p^{*}+\epsilon)-bc}{ab}$ and $y^{*} = \frac{b}{a}$. Hereafter, if $\epsilon = 0$, then normal form for (5.9) is studied. By Taylor series expansion at $(u_n, v_n) = (0, 0)$, from (5.9) one has

$$\begin{aligned} u_{n+1} =& a_{11}u_n + a_{12}v_n + a_{13}u_nv_n, \\ v_{n+1} =& a_{21}u_n + a_{22}v_n + a_{23}u_nv_n, \end{aligned} \tag{5.10}$$

with

$$\begin{aligned} a_{11} &= 1 - bh + ahy^*, \\ a_{12} &= ahx^*, \\ a_{13} &= ah, \\ a_{21} &= -ahy^*, \\ a_{22} &= 1 - ch - ahx^*, \\ a_{23} &= -ah. \end{aligned} \tag{5.11}$$

Hereafter, one construct invertible matrix T that put linear part of (5.10) to required canonical form

$$T := \begin{pmatrix} a_{12} & 0 \\ \eta - a_{11} & -\zeta \end{pmatrix}, \tag{5.12}$$

where

$$\begin{aligned} \eta &= \frac{2b - aph}{2b}, \\ \zeta &= \frac{1}{2}\sqrt{4h^2(ap - bc) - \left(\frac{aph}{b}\right)^2}. \end{aligned} \tag{5.13}$$

Hence, system (5.10) then implies

$$\begin{aligned} X_{n+1} &= \eta X_n - \zeta Y_n + \bar{P}, \\ Y_{n+1} &= \zeta X_n + \eta Y_n + \bar{Q}, \end{aligned} \tag{5.14}$$

with

$$\begin{aligned} \bar{P}(X_n, Y_n) &= l_{11}X_t^2 + l_{12}X_tY_t, \\ \bar{Q}(X_n, Y_n) &= l_{21}X_t^2 + l_{22}X_tY_t, \end{aligned} \tag{5.15}$$

and

$$\begin{aligned} l_{11} &= (\eta - a_{11})a_{13}, \\ l_{12} &= -\zeta a_{13}, \\ l_{21} &= \frac{\eta - a_{11}}{\zeta}\left(a_{13}(\eta - a_{11}) - a_{12}a_{23}\right), \\ l_{22} &= (\eta - a_{11})(a_{12}a_{23} - a_{13}), \end{aligned} \tag{5.16}$$

by

$$\begin{pmatrix} u_n \\ v_n \end{pmatrix} := \begin{pmatrix} a_{12} & 0 \\ \eta - a_{11} & -\zeta \end{pmatrix}\begin{pmatrix} X_t \\ Y_t \end{pmatrix}. \tag{5.17}$$

From (5.15), one gets

$$\begin{aligned} \bar{P}_{X_tX_t}|_{P_{00}(0,0)} =& 2l_{11},\ \bar{P}_{X_tY_t}|_{P_{00}(0,0)} = l_{12}, \\ \bar{P}_{Y_tY_t}|_{P_{00}(0,0)} =& \bar{P}_{X_nX_nX_n}|_{P_{00}(0,0)} = \bar{P}_{X_nX_nY_n}|_{P_{00}(0,0)} \\ =& \bar{P}_{X_nY_nY_n}|_{P_{00}(0,0)} = \bar{P}_{Y_nY_nY_n}|_{P_{00}(0,0)} = 0, \\ \bar{Q}_{X_tX_t}|_{P_{00}(0,0)} =& 2l_{21}, \bar{Q}_{X_tY_t}|_{P_{00}(0,0)} = l_{22}, \\ \bar{Q}_{Y_nY_n}|_{P_{00}(0,0)} =& \bar{Q}_{X_nX_nX_n}|_{P_{00}(0,0)} = \bar{Q}_{X_nX_nY_n}|_{P_{00}(0,0)} \\ =& \bar{Q}_{X_nY_nY_n}|_{P_{00}(0,0)} = \bar{Q}_{Y_nY_nY_n}|_{P_{00}(0,0)} = 0. \end{aligned} \tag{5.18}$$

Now, in order for system (5.14) undergoes Neimark-Sacker bifurcation, it is necessary that $\Omega \neq 0$ (see [14–16]),

$$\Omega = -\Re\left(\frac{(1-2\bar{\lambda})\bar{\lambda}^2}{1-\lambda}\xi_{11}\xi_{20}\right) - \frac{1}{2}\|\xi_{11}\|^2 - \|\xi_{02}\|^2 + \Re(\bar{\lambda}\xi_{21}), \tag{5.19}$$

where

$$\begin{aligned}
\xi_{02} &= \frac{1}{8}\left[\bar{P}_{X_nX_n} - \bar{P}_{Y_nY_n} + 2\bar{Q}_{X_nY_n} + \iota\left(\bar{Q}_{X_nX_n} - \bar{Q}_{Y_nY_n} + 2\bar{P}_{X_nY_n}\right)\right]|_{P_{00}(0,0)},\\
\xi_{11} &= \frac{1}{4}\left[\bar{P}_{X_nX_n} + \bar{P}_{Y_nY_n} + \iota\left(\bar{Q}_{X_nX_n} + \bar{Q}_{Y_nY_n}\right)\right]|_{P_{00}(0,0)},\\
\xi_{20} &= \frac{1}{8}\left[\bar{P}_{X_nX_n} - \bar{P}_{Y_nY_n} + 2\bar{Q}_{X_nY_n} + \iota\left(\bar{Q}_{X_nX_n} - \bar{Q}_{Y_nY_n} - 2\bar{P}_{X_nY_n}\right)\right]|_{P_{00}(0,0)},\\
\xi_{21} &= \frac{1}{16}\left[\bar{P}_{X_nX_nX_n} + \bar{P}_{X_nY_nY_n} + \bar{Q}_{X_nX_nY_n} + \bar{Q}_{Y_nY_nY_n}\right.\\
&\quad \left. + \iota\left(\bar{Q}_{X_nX_nX_n} + \bar{Q}_{X_nY_nY_n} - \bar{P}_{X_nX_nY_n} - P_{Y_nY_nY_n}\right)\right]|_{P_{00}(0,0)}.
\end{aligned} \tag{5.20}$$

After manipulation, one gets

$$\begin{aligned}
\xi_{02} &= \frac{1}{4}\left[l_{11} - l_{22} + \iota(l_{21} + l_{12})\right],\\
\xi_{11} &= \frac{1}{2}\left[l_{11} + \iota l_{21}\right],\\
\xi_{20} &= \frac{1}{4}\left[l_{11} + l_{22} + \iota(l_{21} - l_{12})\right],\\
\xi_{21} &= 0.
\end{aligned} \tag{5.21}$$

So from this analysis and condition(s) for Neimark-Sacker bifurcation discussed in [17, 18], we have the following result about Neimark-Sacker bifurcation of the model (1.4).

Theorem 5.1. If (3.13) holds, then model (1.4) undergoes Neimark-Sacker bifurcation for the fixed point $P^+_{xy}\left(\frac{ap-bc}{ab}, \frac{b}{a}\right)$ as parameters (a, b, c, h, p) goes through the curve (4.2). Additionally, attracting (repelling) closed curve bifurcates from $P^+_{xy}\left(\frac{ap-bc}{ab}, \frac{b}{a}\right)$ if $\Omega < 0$ ($\Omega > 0$).

5.3. Flip bifurcation for $P^+_{xy}(\frac{ap-bc}{ab}, \frac{b}{a})$

Recall that if parameters (a, b, c, h, p) crosses (4.3), then laser model (1.4) undergoes a flip bifurcation. Now if p in a neighborhood of p^*, *i.e*, $p = p^* + \epsilon$ where $\epsilon << 1$, then laser model (1.4) becomes the form (5.1), that further takes the following form:

$$\begin{aligned}
u_{n+1} &= \widehat{a_{11}}u_n + \widehat{a_{12}}v_n + \widehat{a_{13}}u_nv_n,\\
v_{n+1} &= \widehat{a_{21}}u_n + \widehat{a_{22}}v_n + \widehat{a_{23}}u_nv_n + \gamma_{01}\epsilon,
\end{aligned} \tag{5.22}$$

where

$$\begin{aligned}
\widehat{a_{11}} &= 1 - bh + ahy^*, \\
\widehat{a_{12}} &= ahx^*, \\
\widehat{a_{13}} &= ah, \\
\widehat{a_{21}} &= -ahy^*, \\
\widehat{a_{22}} &= 1 - ch - ahx^*, \\
\widehat{a_{23}} &= -ah, \\
\gamma_{01} &= h,
\end{aligned} \tag{5.23}$$

by using transformation given in (5.8). Now (5.22) becomes

$$\begin{pmatrix} X_{n+1} \\ Y_{n+1} \end{pmatrix} = \begin{pmatrix} -1 & 0 \\ 0 & \lambda_2 \end{pmatrix} \begin{pmatrix} X_n \\ Y_n \end{pmatrix} + \begin{pmatrix} \widehat{P} \\ \widehat{Q} \end{pmatrix}, \tag{5.24}$$

where

$$\begin{aligned}
\widehat{P} &= \frac{\widehat{a_{13}}\,(\lambda_2 - \widehat{a_{11}}) - \widehat{a_{12}}\widehat{a_{23}}}{\widehat{a_{12}}\,(1 + \lambda_2)} u_n v_n - \frac{\gamma_{01}}{(1 + \lambda_2)}\epsilon, \\
\widehat{Q} &= \frac{\widehat{a_{13}}\,(1 + \widehat{a_{11}}) + \widehat{a_{12}}\widehat{a_{23}}}{\widehat{a_{12}}\,(1 + \lambda_2)} u_n v_n + \frac{\gamma_{01}}{(1 + \lambda_2)}\epsilon, \\
u_n v_n &= -\widehat{a_{12}}\,(1 + \widehat{a_{11}})\,X_n^2 + (\widehat{a_{12}}\,(\lambda_2 - \widehat{a_{11}}) - \widehat{a_{12}}\,(1 + \widehat{a_{11}}))\,X_n Y_n + \widehat{a_{12}}\,(\lambda_2 - \widehat{a_{11}})\,Y_n^2,
\end{aligned} \tag{5.25}$$

by the transformation

$$\begin{pmatrix} u_n \\ v_n \end{pmatrix} := \begin{pmatrix} \widehat{a_{12}} & \widehat{a_{12}} \\ -1 - \widehat{a_{11}} & \lambda_2 - \widehat{a_{11}} \end{pmatrix} \begin{pmatrix} X_n \\ Y_n \end{pmatrix}. \tag{5.26}$$

Hereafter, for (5.24) center manifold $M^c|_{P_{00}(0,0)}$ at $P_{00}(0,0)$ is explored where

$$M^c|_{P_{00}(0,0)} = \left\{(X_n, Y_n) : Y_n = c_0\epsilon + c_1 X_n^2 + c_2 X_n\epsilon + c_3\epsilon^3 + O\left((|X_n| + |\epsilon|)^3\right)\right\}. \tag{5.27}$$

After manipulations, we obtain

$$\begin{aligned}
c_0 &= \frac{\gamma_{01}}{1 - \lambda_2^2}, \\
c_1 &= -\frac{(1 + \widehat{a_{11}})\,((1 + \widehat{a_{11}})\widehat{a_{13}} + \widehat{a_{12}}\widehat{a_{23}})}{1 - \lambda_2^2}, \\
c_2 &= \frac{\gamma_{01}}{1 - \lambda_2^2}\left(((1 + \widehat{a_{11}})\widehat{a_{13}} + \widehat{a_{12}}\widehat{a_{23}})\,(\lambda_2 - 2\widehat{a_{12}} - 1)\right), \\
c_3 &= 0.
\end{aligned} \tag{5.28}$$

Finally, the map (5.24) restricts to $M^c|_{P_{00}(0,0)}$ is

$$f(x_n) = -x_n + h_1 x_n^2 + h_2 x_n\epsilon + h_3 x_n^2\epsilon + h_4 x_n\epsilon^2 + h_5 x_n^3 + O\left((|X_n| + |\epsilon|)^4\right), \tag{5.29}$$

where

$$
\begin{aligned}
h_1 &= \frac{-(1+\widehat{a_{11}})}{1+\lambda_2}\left[(\lambda_2-\widehat{a_{11}})\,\widehat{a_{13}}-\widehat{a_{12}}\widehat{a_{23}}\right],\\
h_2 &= \frac{c_o(\lambda_2-2\widehat{a_{11}}-1)}{1+\lambda_2}\left[(\lambda_2-\widehat{a_{11}})\,\widehat{a_{13}}-\widehat{a_{12}}\widehat{a_{23}}\right],\\
h_3 &= \frac{\left[(\lambda_2-\widehat{a_{11}})\,\widehat{a_{13}}-\widehat{a_{12}}\widehat{a_{23}}\right]\left[c_2\,(\lambda_2-2\widehat{a_{11}}-1)+2c_oc_1\,(\lambda_2-\widehat{a_{11}})\right]}{1+\lambda_2},\\
h_4 &= \frac{2c_oc_2\,(\lambda_2-\widehat{a_{11}})}{1+\lambda_2}\left[(\lambda_2-\widehat{a_{11}})\,\widehat{a_{13}}-\widehat{a_{12}}\widehat{a_{23}}\right],\\
h_5 &= \frac{c_1(\lambda_2-2\widehat{a_{11}}-1)}{1+\lambda_2}\left[(\lambda_2-\widehat{a_{11}})\,\widehat{a_{13}}-\widehat{a_{12}}\widehat{a_{23}}\right].
\end{aligned}
\tag{5.30}
$$

Thus discriminatory quantities are non-zero in order for (5.29) undergoes flip bifurcation [19–21]

$$
\begin{aligned}
\Gamma_1 &= \left(\frac{\partial^2 f}{\partial x_n\partial\epsilon}+\frac{1}{2}\frac{\partial f}{\partial\epsilon}\frac{\partial^2 f}{\partial x_n^2}\right)|_{P_{00}(0,0)},\\
\Gamma_2 &= \left(\frac{1}{6}\frac{\partial^3 f}{\partial x_n^3}+\left(\frac{1}{2}\frac{\partial^2 f}{\partial x_n^2}\right)^2\right)|_{P_{00}(0,0)}.
\end{aligned}
\tag{5.31}
$$

By computation, we get

$$
\Gamma_1 = \frac{ah(2-bh)^2(bch^2-4)}{(4-4bh+bch^2)\,(b^2c^2h^2-4bc+2b^2ch^2)}\left(\frac{bch-2b}{2-bh}+\frac{ap-bc}{b}\right),
\tag{5.32}
$$

and

$$
\begin{aligned}
\Gamma_2 = {} & \frac{-2a\left(2ah-\frac{ah^2(ap-bc)}{b}\right)\left(\frac{bch^2-4}{2-bh}\right)\left(bch^2-4\right)\left(\frac{bch-2b}{2-bh}+\frac{ap-bc}{b}\right)}{(4-4bh+bch^2)\,(b^2c^2h^2-4bc+2b^2ch^2)}\\
& +\frac{4\,(2-bh)^2\,a^2h^4}{(4-4bh+bch^2)^2}\left(\frac{bch-2b}{2-bh}+\frac{ap-bc}{b}\right)^2.
\end{aligned}
\tag{5.33}
$$

From this analysis, we have the following theorem.

Theorem 5.2. For $P_{xy}^{+}\left(\frac{ap-bc}{ab},\frac{b}{a}\right)$, map (5.1) undergoes a flip bifurcation if ϵ varies in a small neighborhood of $P_{00}(0,0)$. Moreover, if $\Gamma_2 > 0$ ($\Gamma_2 < 0$), then period-2 orbits bifurcate from $P_{xy}^{+}\left(\frac{ap-bc}{ab},\frac{b}{a}\right)$ are stable (unstable).

6. Numerical simulations

In this section, obtained theoretical results are illustrated numerically. Let $a = 0.5$, $b = 1.6$, $c = 0.03$, $h = 1.12$, then from (3.13) one gets $p = 0.217212$. In this case, $P_{xy}^{+}\left(\frac{ap-bc}{ab},\frac{b}{a}\right)$ of (1.4) is a stable focus if $p < 0.217212$, loss its stability if $p = 0.217212$ and meanwhile it is an unstable focus if $p > 0.217212$. For this, if $p = 0.11 < 0.217212$, then from Figure 1a it is clear that $P_{xy}^{+}\left(\frac{d}{c},\frac{r(c-d)}{bc}\right)$=$P_{xy}^{+}\,(0.07575757575757576, 3.2)$ of laser model (1.4) is a stable focus.

Correspondingly, for the remaining values of p, if $p < 0.217212$, then, respective equilibrium point is also a stable focus (Figure 1b–1l). But if $p = 0.217212$, then $P^{+}_{xy}(\frac{ap-bc}{ab}, \frac{b}{a})$ change the behavior and thus an unstable focus if $p > 0.217212$, and as a consequence, stable curve appears, which indicates that laser model (1.4) undergoes supercritical Neimark-Sacker bifurcation. To prove this, if $p = 0.217222 > 0.217212$, then roots of $J_{P^{+}_{xy}\left(\frac{ap-bc}{ab}, \frac{b}{a}\right)}$ evaluated at $P^{+}_{xy}\left(\frac{ap-bc}{ab}, \frac{b}{a}\right)$ are

$$\lambda_{1,2} = 0.961986 \pm 0.273103\iota. \tag{6.1}$$

Moreover, from (5.7) one gets $\frac{bch}{2(bh-1)} = 0.033939393939393936 > 0$. After some manipulation, from (5.21) one gets

$$\begin{aligned} \xi_{02} &= 0.000225798 + 0.0381484\iota, \\ \xi_{11} &= -0.0106439 - 0.000172025\iota, \\ \xi_{20} &= -0.0108697 - 0.0383205\iota, \\ \xi_{21} &= 0. \end{aligned} \tag{6.2}$$

Using (6.1) and (6.2) in (5.19), we obtain $\Omega = -0.0016523767625482892 < 0$. Hence, laser model (1.4) undergoes supercritical a Neimark-Sacker bifurcation if $p = 0.217222 > 0.217212$ and meanwhile stable curve appear (Figure 2a). Similarly, if $p > 0.217212$, then $\Omega < 0$ (See Table 1) and their corresponding closed curves are drawn in Figure 2b–2l. Moreover, M.L.E and bifurcation diagrams are drawn in Figure 3. Finally, bifurcation diagrams in $3D$ are presented in Figure 4.

Hereafter, we will give simulation in order to validate obtained results in Section 5.3 by fixing $a = 1.13, b = 1.012,\ c = 1.5$ and $0.02 \leq p \leq 4.9$. If $a = 1.13, b = 1.012,\ c = 1.5$, then from (3.16) one gets $p = 1.72336$. So, $P^{+}_{xy}\left(\frac{ap-bc}{ab}, \frac{b}{a}\right) = P^{+}_{xy}(0.375491, 0.895575)$ is a stable node if $p < 1.72336$, non-hyperbolic if $p = 1.72336$, an unstable node if $p > 1.72336$, and thus flip bifurcation exists if $p > 1.72336$. Figure 5a and 5b indicates that fixed point is a stable if $p < 1.72336$ and loss stability at $p = 1.72336$. Now corresponding to Figure 5a and 5b, M.L.E are drawn in Figure 5c. Additionally $3D$ flip bifurcation diagrams equivalent to Figure 5a and 5b are presented in Figure 6a–6h. Finally, more plots of laser model (1.4) that related with Figure 5a and 5b are drawn in Figure 7a–7f, that shows model (1.4) yields a complex dynamics having orbits of period -2, -3, -4, -5, -8 and -9.

Table 1. Numerical values of Ω for $p > 0.217212$.

Bifurcation values if $p > 0.217212$	Values of Ω
0.217222	$-0.0016523767625482892 < 0$
0.2172124	$-0.0016523096396154336 < 0$
0.217412	$-0.001653861096012872 < 0$
0.217612	$-0.0016549900334033758 < 0$
0.220	$-0.0016707992836875582 < 0$
0.217812	$-0.0016563267520259238 < 0$
0.2179912	$-0.0016575224832815231 < 0$
0.21889	$-0.0016634917766999676‘ < 0$
0.219	$-0.0016642191214841734 < 0$
0.2189	$-0.0016635579278594646 < 0$
0.218899	$-0.001663551313003689 < 0$
0.21889	$-0.0016634917766999676 < 0$

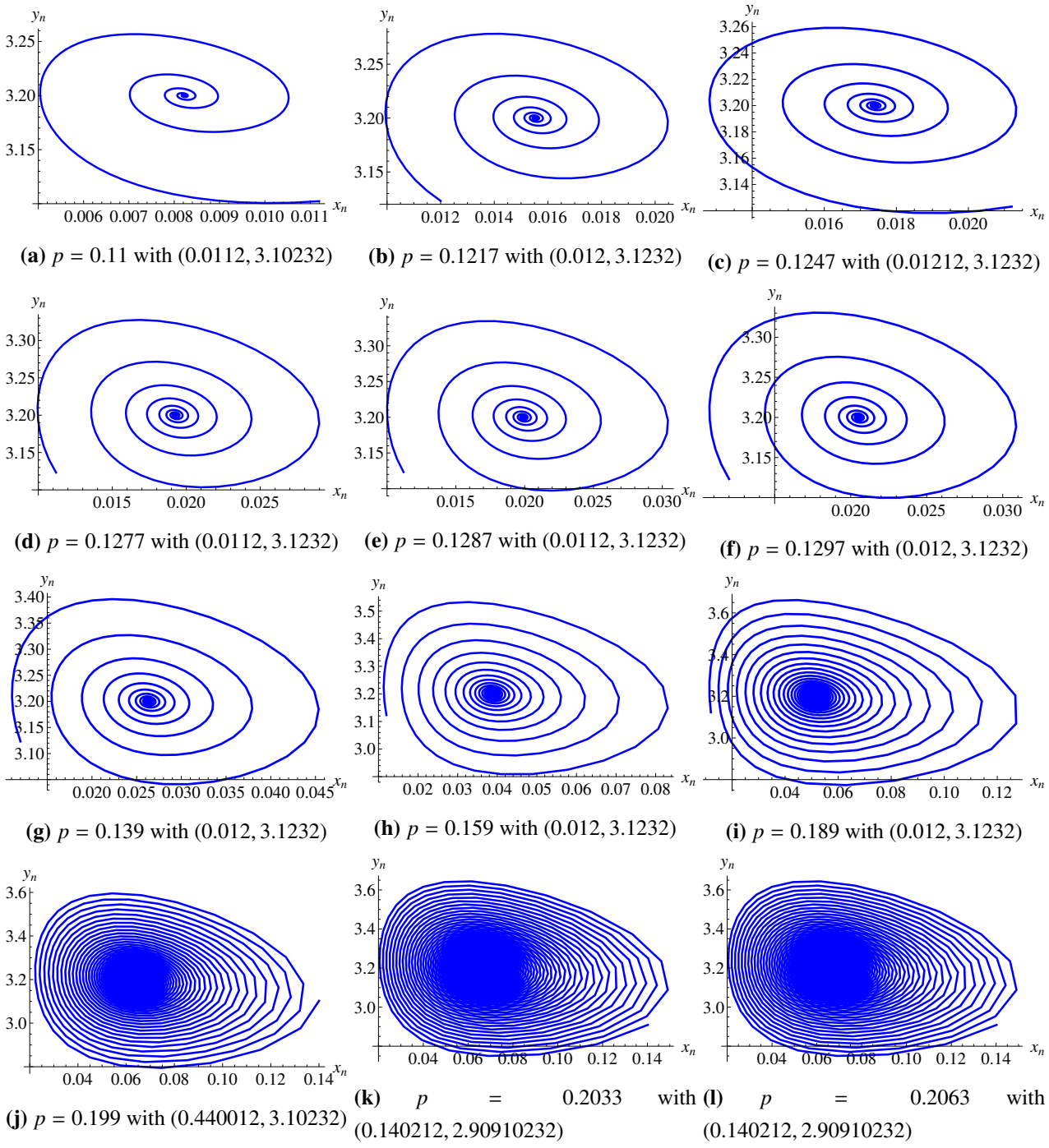

(a) $p = 0.11$ with $(0.0112, 3.10232)$ **(b)** $p = 0.1217$ with $(0.012, 3.1232)$ **(c)** $p = 0.1247$ with $(0.01212, 3.1232)$

(d) $p = 0.1277$ with $(0.0112, 3.1232)$ **(e)** $p = 0.1287$ with $(0.0112, 3.1232)$ **(f)** $p = 0.1297$ with $(0.012, 3.1232)$

(g) $p = 0.139$ with $(0.012, 3.1232)$ **(h)** $p = 0.159$ with $(0.012, 3.1232)$ **(i)** $p = 0.189$ with $(0.012, 3.1232)$

(j) $p = 0.199$ with $(0.440012, 3.10232)$ **(k)** $p = 0.2033$ with $(0.140212, 2.90910232)$ **(l)** $p = 0.2063$ with $(0.140212, 2.90910232)$

Figure 1. Phase portrait for the laser model (1.4).

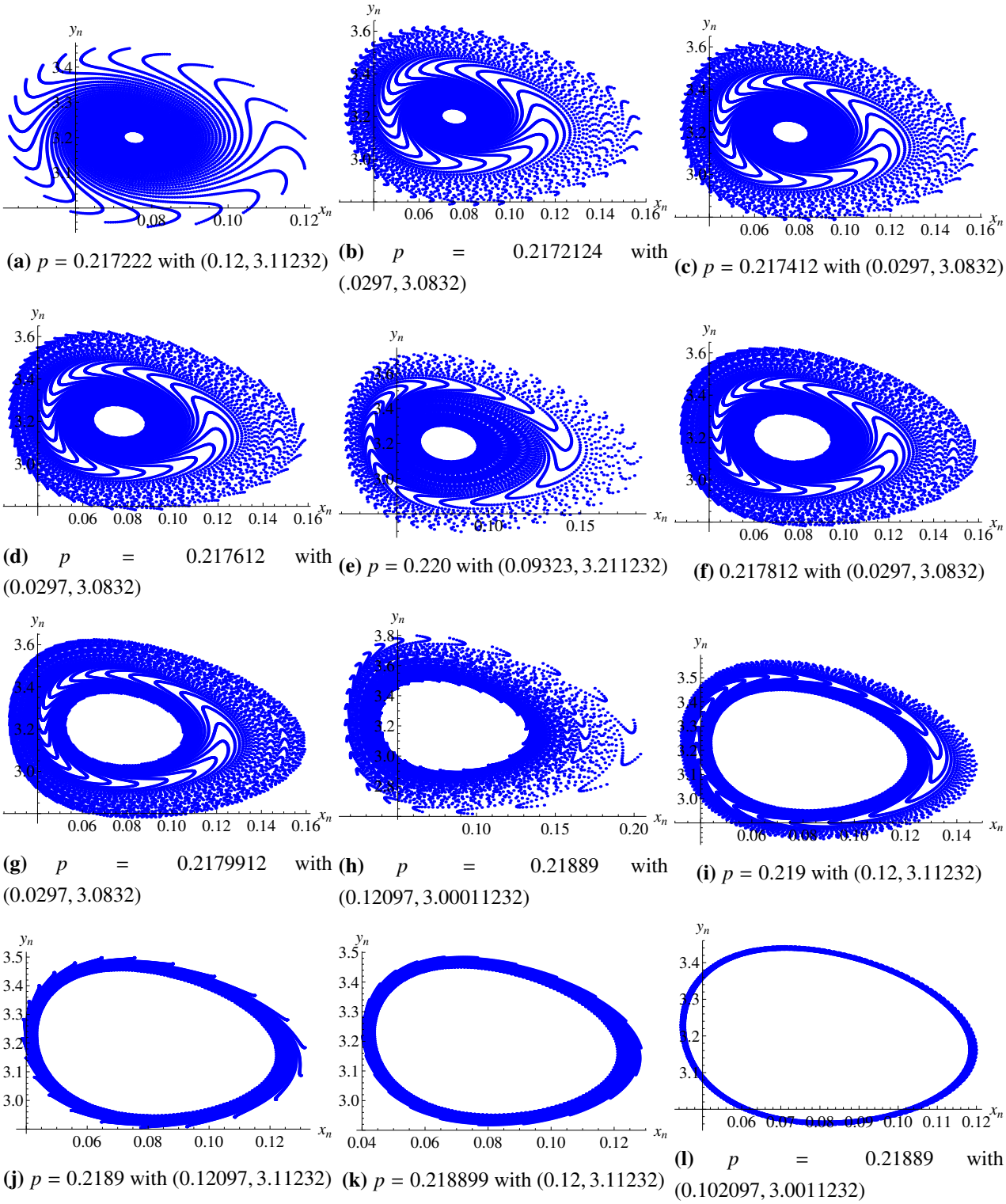

(a) $p = 0.217222$ with $(0.12, 3.11232)$ **(b)** $p = 0.2172124$ with $(.0297, 3.0832)$ **(c)** $p = 0.217412$ with $(0.0297, 3.0832)$

(d) $p = 0.217612$ with $(0.0297, 3.0832)$ **(e)** $p = 0.220$ with $(0.09323, 3.211232)$ **(f)** 0.217812 with $(0.0297, 3.0832)$

(g) $p = 0.2179912$ with $(0.0297, 3.0832)$ **(h)** $p = 0.21889$ with $(0.12097, 3.00011232)$ **(i)** $p = 0.219$ with $(0.12, 3.11232)$

(j) $p = 0.2189$ with $(0.12097, 3.11232)$ **(k)** $p = 0.218899$ with $(0.12, 3.11232)$ **(l)** $p = 0.21889$ with $(0.102097, 3.0011232)$

Figure 2. Closed curves of the laser model (1.4).

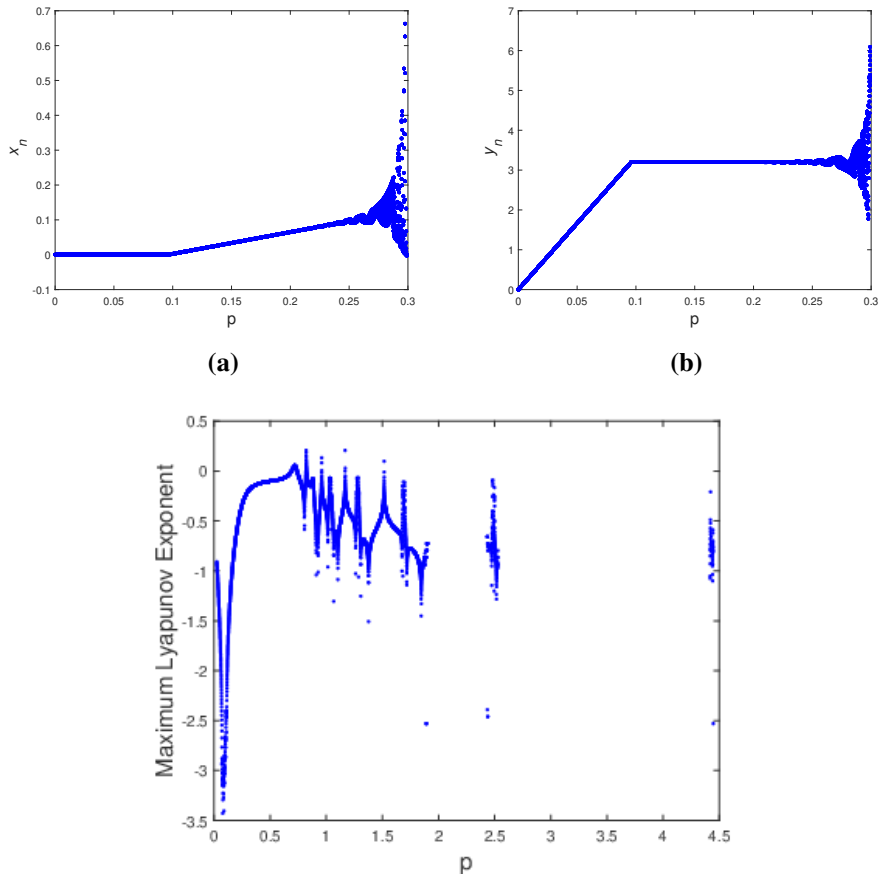

(a) **(b)**

(c)

Figure 3. Bifurcation diagram and their corresponding M.L.E of laser model (1.4) for $P^{+}_{xy}\left(\frac{ap-bc}{ab}, \frac{b}{a}\right)$. (a, b) Bifurcation diagram of (1.4) if $0.000089 \leq p \leq 0.47$ and initial condition $(0.00549, 4.037654)$. (c) M.L.E corresponding to (a) and (b).

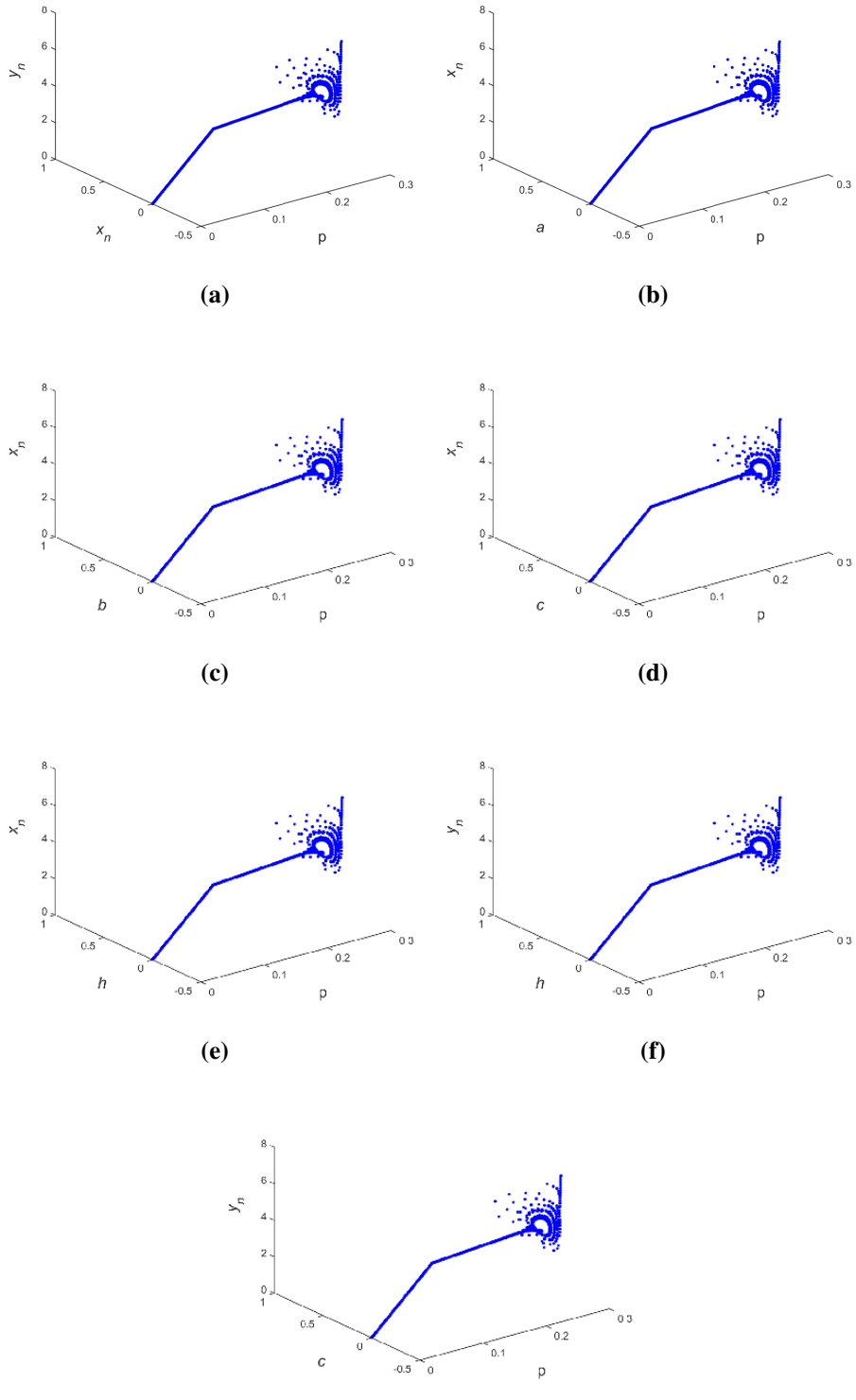

Figure 4. 3*D* bifurcation diagrams.

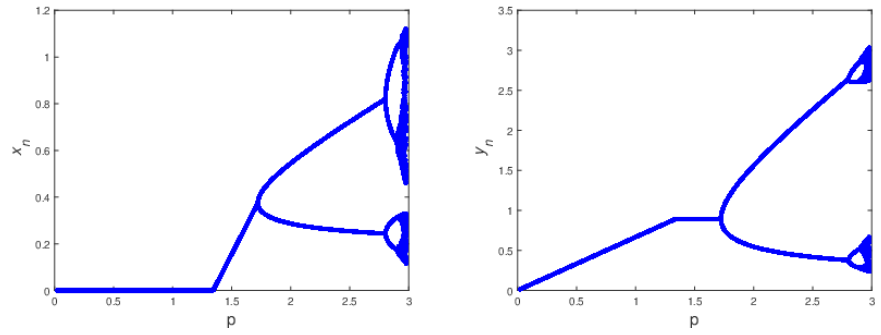

(a) **(b)**

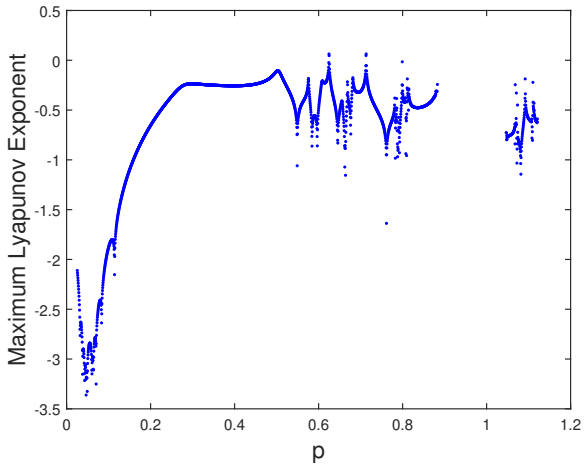

(c)

Figure 5. Bifurcation diagram and their corresponding M.L.E of (1.4) for $P^{+}_{xy}\left(\frac{ap-bc}{ab}, \frac{b}{a}\right)$. (a, b) Bifurcation diagram of the model if $0.02 \leq p \leq 4.9$ and $(0.712, 0.4)$. (c) M.L.E corresponding to (a) and (b).

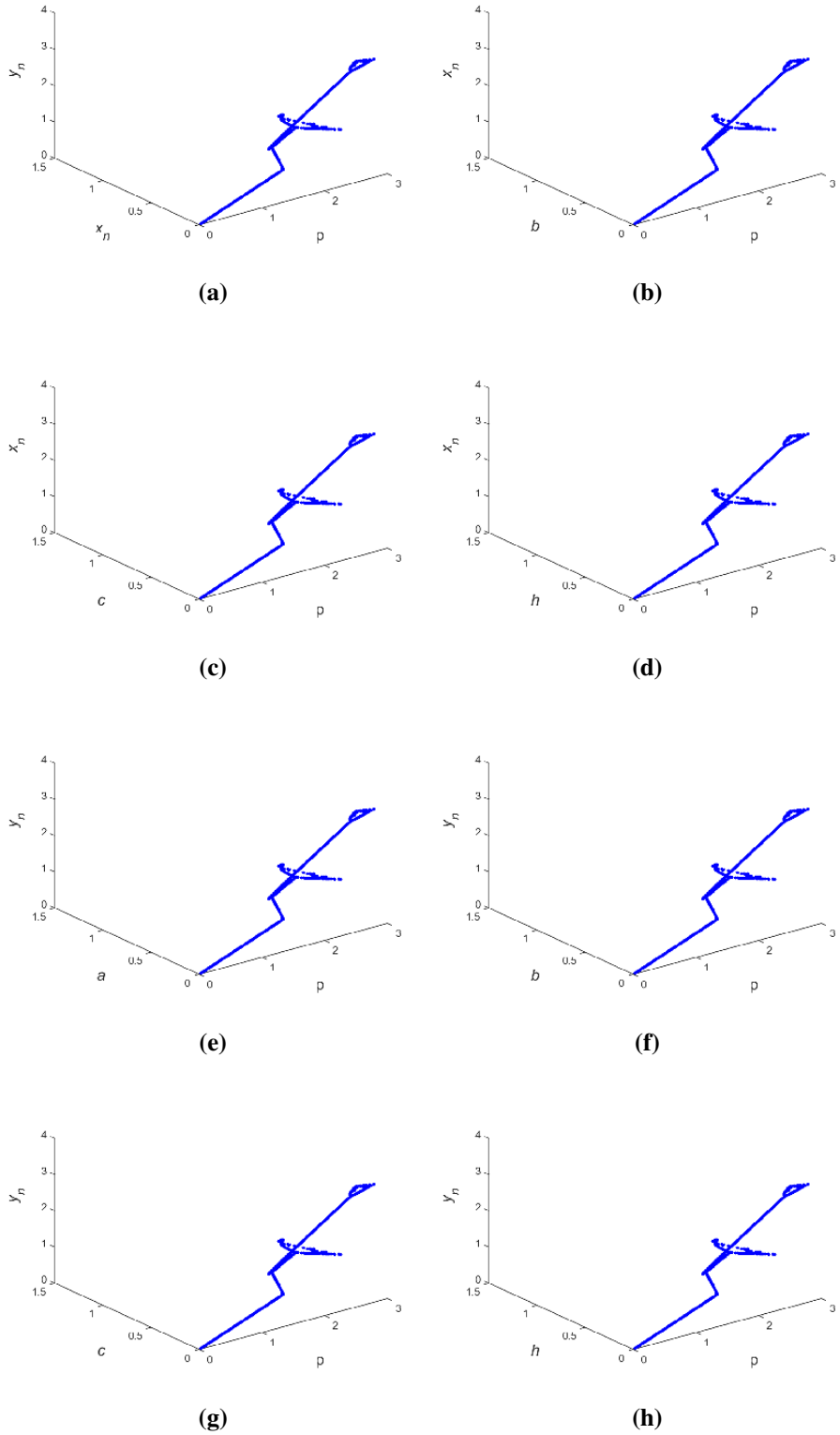

Figure 6. 3*D* flip bifurcation diagrams of the model (1.4).

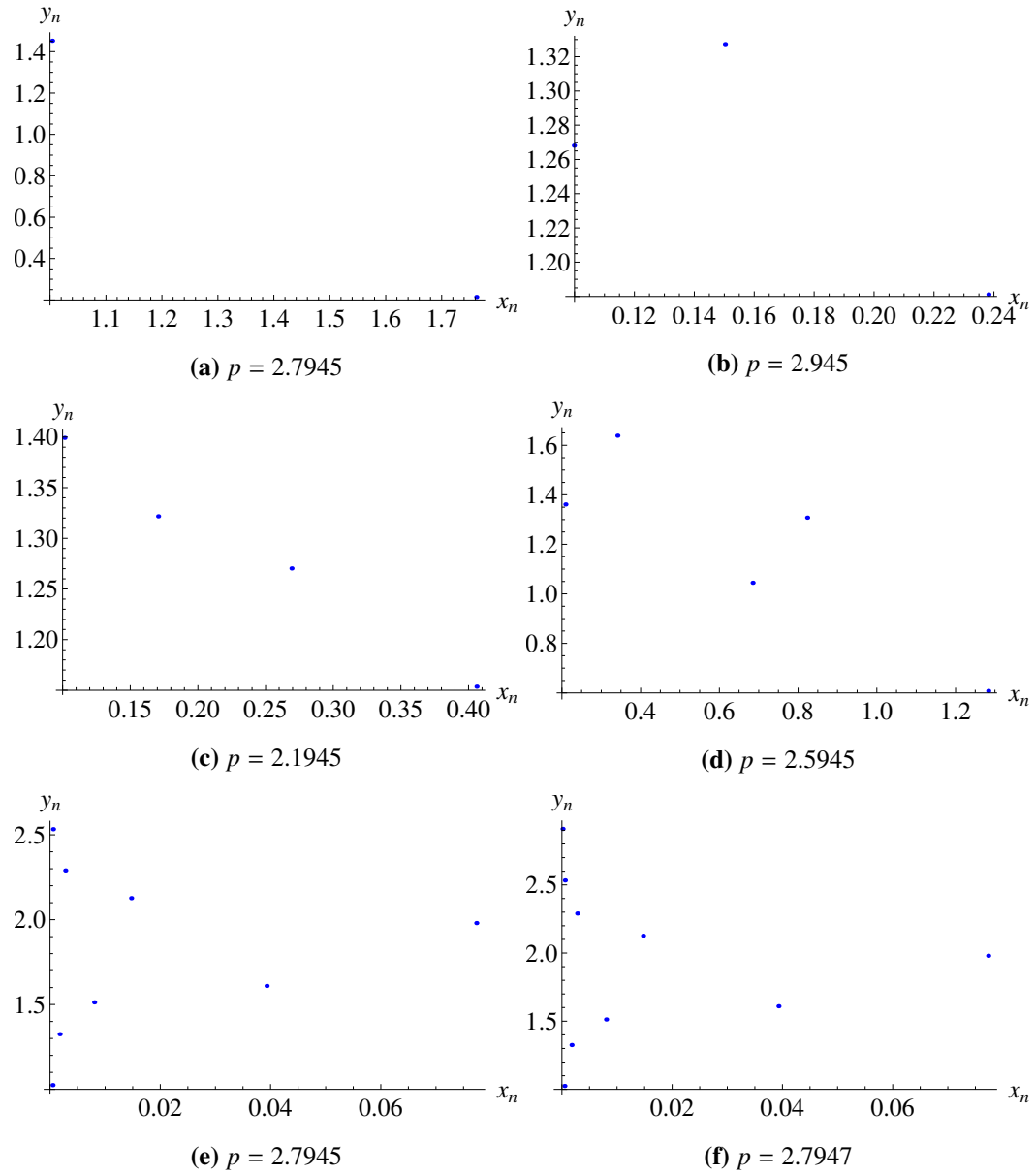

(a) $p = 2.7945$ **(b)** $p = 2.945$ **(c)** $p = 2.1945$ **(d)** $p = 2.5945$ **(e)** $p = 2.7945$ **(f)** $p = 2.7947$

Figure 7. Complex dynamics behaviors of (1.4).

6.1. Fractal dimension

The strange attractors designated by fractal dimension for discrete system takes the following form [22, 23]:

$$d_L = l + \frac{\sum_{j=1}^{l} \lambda_l}{|\lambda_l|}, \tag{6.3}$$

where Lyapunov exponents are λ_i $(i = 1, \cdots, n)$ and l is the largest integer for which $\sum_{j=1}^{l} \lambda_l \geq 0$ and $\sum_{j=1}^{l+1} \lambda_l < 0$. For the model (1.4), (6.3) becomes

$$d_L = 1 + \frac{\lambda_1}{|\lambda_2|}, \ \lambda_1 > 0 > \lambda_2. \tag{6.4}$$

Fixing $a = 1.13$, $b = 1.012$, $c = 1.5$, $h = 1.2$, then two Lyapunov exponents are commuted numerically, and one gets $\lambda_1 = 0.647622569300813$ ($\lambda_1 = 0.5786643421204638$) and $\lambda_2 = -1.0393814625814453$ ($\lambda_2 = -1.1111149350058382$) if $p = 1.785$ ($p = 1.89$). The fractal dimension for (1.4) becomes

$$\begin{aligned} d_L &= 1 + \frac{0.647622569300813}{1.0393814625814453} = 1.6230858781196482 \text{ for } p = 1.785, \\ d_L &= 1 + \frac{0.5786643421204638}{1.1111149350058382} = 1.5208028080280802 \text{ for } p = 1.89. \end{aligned} \tag{6.5}$$

Finally, for above chosen values, strange attractors are also plotted in Figure 8a and 8b, which shows that (1.4) gives complex dynamics if p increases.

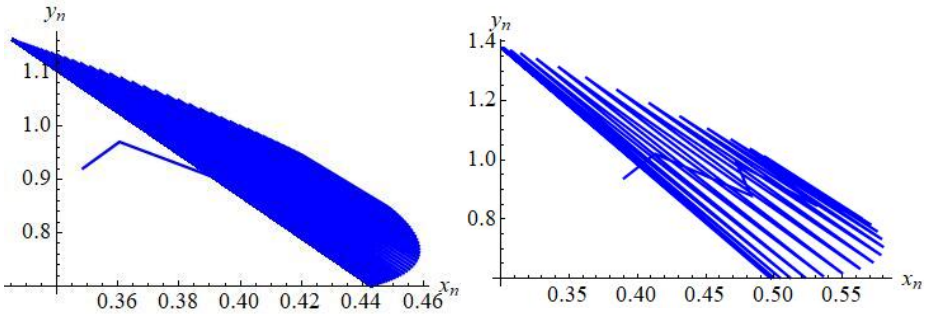

(a) **(b)**

Figure 8. Strange attractor of (1.4) if $p = 1.785$ ($p = 1.89$) with (0.040, 1.04).

7. Chaos control

We explore chaos control by utilizing state feedback control method [24, 25] in this section. On adding u_n as a control force to (1.4), one has

$$\begin{aligned} x_{n+1} &= (1 - bh)\, x_n + ahx_n y_n + u_n, \\ y_{n+1} &= (1 - ch)\, y_n - ahx_n y_n + ph. \end{aligned} \tag{7.1}$$

The control force depicted in (7.1) given by

$$u_n = -l_1(x_n - x^*) - l_2(y_n - y^*), \tag{7.2}$$

where l_1 and l_2 denotes feedback gains, and $x^* = \frac{ap-bc}{ab}$ and $y^* = \frac{b}{a}$. The $JC|_{P_{xy}(x^*,y^*)}$ of (7.1) is

$$JC|_{P_{xy}(x^*,y^*)} = \begin{pmatrix} n_{11} - l_1 & n_{12} - l_2 \\ n_{21} & n_{22} \end{pmatrix}, \tag{7.3}$$

where

$$\begin{aligned} n_{11} &= 1, \\ n_{12} &= \frac{aph - bch}{b}, \\ n_{21} &= -bh, \\ n_{22} &= \frac{b - aph}{b}. \end{aligned} \tag{7.4}$$

Moreover, characteristic equation of $JC|_{P_{xy}(x^*,y^*)}$ evaluated at $P_{xy}(x^*, y^*)$ is

$$\lambda^2 - tr\left(JC|_{P_{xy}(x^*,y^*)}\right)\lambda + det\left(JC|_{P_{xy}(x^*,y^*)}\right) = 0, \tag{7.5}$$

where

$$\begin{aligned} tr\left(JC|_{P_{xy}(x^*,y^*)}\right) &= n_{11} + n_{22} - l_1, \\ det\left(JC|_{P_{xy}(x^*,y^*)}\right) &= n_{22}(n_{11} - l_1) - n_{21}(n_{12} - l_2). \end{aligned} \tag{7.6}$$

If $\lambda_{1,2}$ are roots of (7.5), then

$$\lambda_1 + \lambda_2 = n_{11} + n_{22} - l_1, \tag{7.7}$$

and

$$\lambda_1\lambda_2 = n_{22}(n_{11} - l_1) - n_{21}(n_{12} - l_2). \tag{7.8}$$

Now lines of marginal stability determines from the solution of $\lambda_1 = \pm 1$ and $\lambda_1\lambda_2 = 1$, which confirm that $|\lambda_{1,2}| < 1$. If $\lambda_1\lambda_2 = 1$, then from (7.8), one gets

$$L_1 : \left(1 - \frac{aph}{b}\right)(1 - l_1) + aph^2 - bch^2 - bhl_2 - 1 = 0. \tag{7.9}$$

If $\lambda_1 = 1$, then from (7.7) and (7.8) one gets

$$L_2 : \frac{aph}{b}l_1 + aph^2 - bch^2 - bhl_2 = 0. \tag{7.10}$$

Finally if $\lambda_1 = -1$, then from (7.7) and (7.8) one gets

$$L_3 : (2 - l_1)(2b - aph) + bh(aph - bch - bl_2) = 0. \tag{7.11}$$

Hence L_1, L_2 and L_3 in (l_1, l_2)-plane gives a triangular region which give $|\lambda_{1,2}| < 1$ (Figure 9a).

To justify how this method works and also control chaos at unstable state, we presented simulation. Figure 9b and 9c shows that for $P^+_{xy}(\frac{ap-bc}{ab}, \frac{b}{a})$ the chaotic trajectories is stabilized.

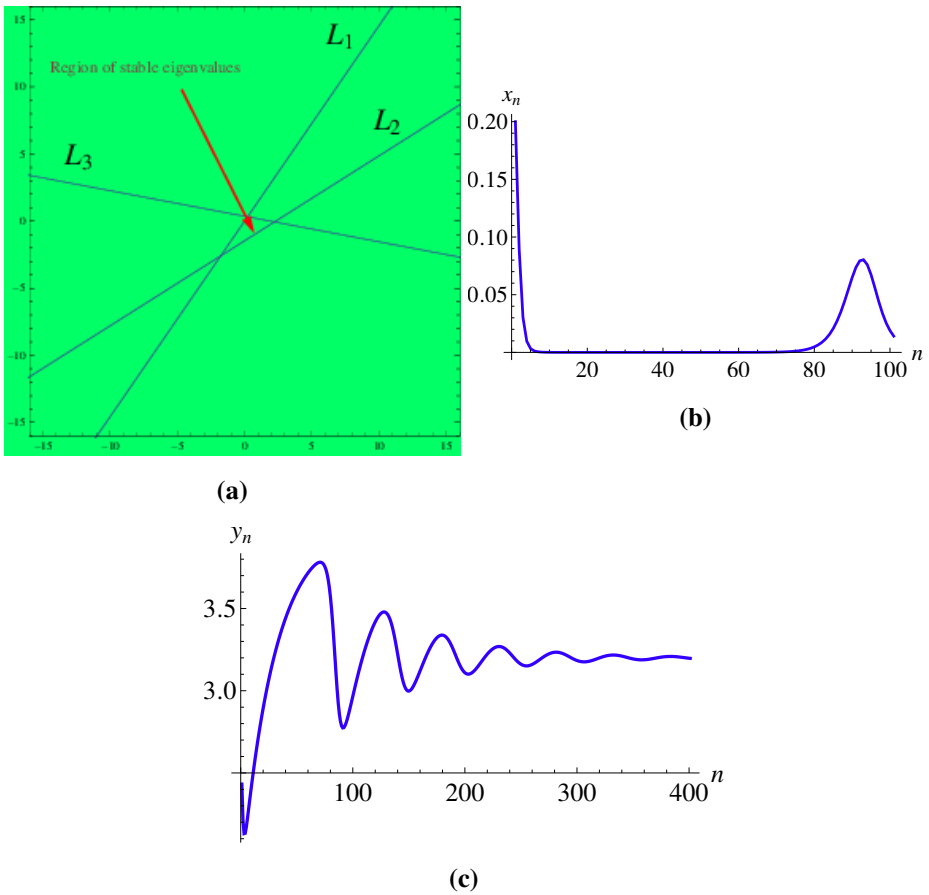

Figure 9. Control of chaotic trajectories of (7.1) for $a = 1.13$, $b = 1.012$, $c = 2.4$, $h = 1.2$, $p = 1.32$ with $(0.01, 0.723)$, (a) Stability region in (l_1, l_2)-plan. (b, c) Behavior for x_n and y_n, respectively.

8. Conclusions

We have explored the local dynamical properties, bifurcations and chaos in the laser model (1.4) in the interior of $\mathbb{R}^2_+$. We have explored that for all parametric values, model (1.4) has a boundary equilibrium $P_{0y}\left(0, \frac{p}{c}\right)$ and if $p > \frac{bc}{a}$ then it has a unique positive equilibrium point $P^+_{xy}\left(\frac{ap-bc}{ab}, \frac{b}{a}\right)$. By linear stability theory, local dynamics with different topological classifications for fixed points $P_{0y}\left(0, \frac{p}{c}\right)$ and $P^+_{xy}\left(\frac{ap-bc}{ab}, \frac{b}{a}\right)$ are studied, and main finding are presented in Table 2. We have also explored existence of possible bifurcations for fixed points $P_{0y}\left(0, \frac{p}{c}\right)$ and $P^+_{xy}\left(\frac{ap-bc}{ab}, \frac{b}{a}\right)$. By computation, it is proved that for $P_{0y}\left(0, \frac{p}{c}\right)$ discrete model (1.4) cannot undergoes a flip bifurcation when parameters (a, b, c, h, p) goes through the curve (4.1). But for $P^+_{xy}\left(\frac{ap-bc}{ab}, \frac{b}{a}\right)$, laser model (1.4) undergoes both Neimark-Saker and flip bifurcations when (a, b, c, h, p) respectively goes through the parametric curves (4.2) and (4.3). It is important here to mention that the existence of Neimark-Sacker bifurcation for the unique positive equilibrium point $P^+_{xy}\left(\frac{ap-bc}{ab}, \frac{b}{a}\right)$ of discrete laser model (1.4) means that there exists a periodic or quasi-periodic oscillations between laser photon and number of atom in the excited state. Some numerical simulations have been implemented to validate not only obtain results but also exhibit complex dynamics of period -2, -3, -4, -5, -8 and -9. The M.L.E as well as

fractal dimension has computed numerically to validate chaotic behaviors of the laser model. Finally, feedback control method is applied to stabilized chaos exists in laser model (1.4). The chaos control and bifurcation analysis of a discrete fractional-order laser model are our next aim to study.

Table 2. Fixed points $P_{0y}\left(0, \frac{p}{c}\right)$ and $P^{+}_{xy}\left(\frac{ap-bc}{ab}, \frac{b}{a}\right)$ along their behavior of model (1.4).

Fixed points	Corresponding behavior
$P_{0y}\left(0, \frac{p}{c}\right)$	sink if $p > \frac{bch-2c}{ah}$ and $c < \frac{2}{h}$; source if $p < \frac{bch-2c}{ah}$ and $c > \frac{2}{h}$; saddle if $p < \frac{bch-2c}{ah}$ and $c < \frac{2}{h}$; non-hyperbolic if $p = \frac{bch-2c}{ah}$ or $c = \frac{2}{h}$.
$P^{+}_{xy}\left(\frac{ap-bc}{ab}, \frac{b}{a}\right)$	locally asymptotically stable focus if $p < \frac{hb^2c}{a(bh-1)}$; an unstable focus if $p > \frac{hb^2c}{a(bh-1)}$; non-hyperbolic if $p = \frac{hb^2c}{a(bh-1)}$; locally asymptotically stable node if $p < \frac{b\left(4-bh^2c\right)}{ah(2-bh)}$; an unstable node if $p > \frac{b\left(4-bh^2c\right)}{ah(2-bh)}$; non-hyperbolic if $p = \frac{b\left(4-bh^2c\right)}{ah(2-bh)}$.

Acknowledgments

This work was partially supported by the Higher Education Commission (HEC) of Pakistan.

Conflict of interest

The authors declare that they have no conflicts of interest regarding the publication of this paper.

References

1. J. C. Ion, *Laser processing of engineering materials: principles, procedure and industrial application*, Elsevier, 2005.
2. Z. X. Guo, S. Kumar, Discrete-ordinates solution of short-pulsed laser transport in two-dimensional turbid media, *Appl. Opt.*, **40** (2001), 3156–3163. https://doi.org/10.1364/AO.40.003156
3. X. Y. Jiang, C. M. Soukoulis, Time dependent theory for random lasers, *Phys. Rev. Lett.*, **85** (2000), 70. https://doi.org/10.1103/PhysRevLett.85.70
4. A. R. Jha, *Infrared technology: applications to electro-optics, photonic devices and sensors*, New York: Wiley, 2000.

5. B. A. Lengyel, *Introduction to laser physics*, New York: Wiley, 1966.
6. J. Ohtsubo, *Semiconductor lasers: stability, instability and chaos*, Berlin, Heidelberg: Springer, 2013. https://doi.org/10.1007/978-3-642-30147-6
7. M. J. Weber, Science and technology of laser glass, *J. Non-Cryst. Solids*, **123** (1990), 208–222. https://doi.org/10.1016/0022-3093(90)90786-L
8. P. W. Milonni, J. H. Eberly, *Lasers physics*, New York: Wiley, 2010. https://doi.org/10.1002/9780470409718
9. H. Haken, *Synergetics*, Berlin, Heidelberg: Springer, 1983. https://doi.org/10.1007/978-3-642-88338-5
10. S. H. Strogatz, *Nonlinear dynamics and chaos with student solutions manual: with applications to physics, biology, chemistry, and engineering*, Boca Raton: CRC Press, 2018. https://doi.org/10.1201/9780429399640
11. J. Guckenheimer, P. Holmes, *Nonlinear oscillations, dynamical systems and bifurcation of vector fields*, New York: Springer, 1983. https://doi.org/10.1007/978-1-4612-1140-2
12. Y. A. Kuznetsov, *Elements of applied bifurcation theorey*, New York: Springer, 2004. https://doi.org/10.1007/978-1-4757-3978-7
13. Z. Y. Hu, Z. D. Teng, L. Zhang, Stability and bifurcation analysis of a discrete predator-prey model with nonmonotonic functional response, *Nonlinear Anal. Real World Appl.*, **12** (2011), 2356–2377. https://doi.org/10.1016/j.nonrwa.2011.02.009
14. A. Q. Khan, J. Y. Ma, D. M. Xiao, Bifurcations of a two-dimensional discrete time plant-herbivore system, *Commun. Nonlinear Sci. Numer. Simul.*, **39** (2016), 185–198. https://doi.org/10.1016/j.cnsns.2016.02.037
15. A. Q. Khan, J. Y. Ma, D. M. Xiao, Global dynamics and bifurcation analysis of a host-parasitoid model with strong Allee effect, *J. Biol. Dyn.*, **11** (2017), 121–146. https://doi.org/10.1080/17513758.2016.1254287
16. Z. J. Jing, J. P. Yang, Bifurcation and chaos in discrete-time predator-prey system, *Chaos Solitons Fract.*, **27** (2006), 259–277. https://doi.org/10.1016/j.chaos.2005.03.040
17. C. H. Zhang, X. P. Yan, G. H. Cui, Hopf bifurcations in a predator-prey system with a discrete delay and a distributed delay, *Nonlinear Anal. Real World Appl.*, **11** (2010), 4141–4153. https://doi.org/10.1016/j.nonrwa.2010.05.001
18. M. Sen, M. Banerjee, A. Morozov, Bifurcation analysis of a ratio-dependent prey-predator model with the Allee effect, *Ecol. Complex.*, **11** (2012), 12–27. https://doi.org/10.1016/j.ecocom.2012.01.002
19. C. D. Huang, J. Wang, X. P. Chen, J. D. Cao, Bifurcations in a fractional-order BAM neural network with four different delays, *Neural Netw.*, **141** (2021), 344–354. https://doi.org/10.1016/j.neunet.2021.04.005
20. E. Kaslik, I. R. Radulescu, Stability and bifurcations in fractional-order gene regulatory networks, *Appl. Math. Comput.*, **421** (2022), 126916. https://doi.org/10.1016/j.amc.2022.126916
21. J. Alidousti, Stability and bifurcation analysis for a fractional prey-predator scavenger model, *Appl. Math. Model.*, **81** (2020), 342–355. https://doi.org/10.1016/j.apm.2019.11.025

22. J. H. E. Cartwright, Nonlinear stiffness, Lyapunov exponents, and attractor dimension, *Phys. Lett. A*, **264** (1999), 298–302. https://doi.org/10.1016/S0375-9601(99)00793-8

23. J. L. Kaplan, J. A. Yorke, Preturbulence: a regime observed in a fluid flow model of Lorenz, *Commun. Math. Phys.*, **67** (1979), 93–108. https://doi.org/10.1007/BF01221359

24. S. N. Elaydi, *An introduction to difference equations*, New York: Springer, 1996. https://doi.org/10.1007/978-1-4757-9168-6

25. S. Lynch, *Dynamical systems with applications using Mathematica*, Boston: Birkhäuser, 2007.

AIMS Press